Competition of zinc(II) with cadmium(II) or mercury(II) in binding to a 12-mer peptide

Attila Jancsó,[a,b*] Béla Gyurcsik,[a,b] Edit Mesterházy,[a] Róbert Berkecz[c]

[a] *Department of Inorganic and Analytical Chemistry, University of Szeged, Dóm tér 7, Szeged, H-6720, Hungary*

[b] *Bioinorganic Chemistry Research Group of the Hungarian Academy of Sciences, University of Szeged, Dóm tér 7, Szeged, H-6720, Hungary*

[c] *Department of Medical Chemistry, University of Szeged, Dóm tér 8, Szeged, H-6720, Hungary*

[*] Corresponding author:

Attila Jancsó: jancso@chem.u-szeged.hu , Tel.: +36 62 544 335 , fax: +36 62 54 43 40

Abstract

Speciation of the complexes of zinc(II) with a dodecapeptide (Ac-SCPGDQGSDCSI-NH_2), inspired by the metal binding domain of MerR metalloregulatory proteins, have been studied by pH-potentiometric titrations, UV, SRCD (synchrotron radiation circular dichroism) and ^{1}H NMR experiments. (MerR is a family of transcriptional regulators the archetype of which is the Hg^{2+}-responsive transcriptional repressor-activator MerR protein.) The aim of the ligand-design was to retain the advantageous metal binding features of MerR proteins in a model peptide for the efficient capture of toxic metal ions. The peptide binds zinc(II) via two deprotonated Cys-thiol groups and one of the Asp-carboxylates in the ZnL parent complex, possessing a remarkably high stability (log$K$ = 9.93). In spite of the relatively long peptide loop, bis-complexes are also formed with the metal ion under basic conditions. In a competition with cadmium(II) or mercury(II), zinc(II) cannot prevent the binding of toxic metal ions by the thiolate donor groups of the ligand. Around neutral pH one equivalent of mercury(II) was shown to fully replace zinc(II) from the ZnL species. Partial replacement of zinc(II) from the peptide by one equivalent of cadmium(II), relative to zinc(II) and the ligand, is also presumable, nevertheless, spectroscopic data may suggest the formation of mixed metal ion complexes, as well. Based on the obtained results the investigated dodecapeptide can be a promising candidate for capturing toxic metal ions in practical applications.

Keywords: Toxic metal ions; Zinc(II); Peptide complexes; Competition; Solution studies

1. Introduction

Nondegradable heavy metal contaminants appear in the environment [1] from natural or non-natural sources. Depending on the exposure level or chemical form, these pollutants may have adverse impacts on the environment and present a hazard for living organisms [2–

5]. Consequently, there is a growing need for the detection, monitoring and removal of toxic metal constituents from contaminated media [4, 5]. The attributes for these techniques may overlap if preconcentration methodologies are required for assisting analytical detection [5]. Although there are efficient and sensitive analytical methods for the determination of low level metal ion concentrations, these techniques often suffer from the need of laboratory-bound expensive equipments and highly skilled personnel [6–8]. The drawbacks of physicochemical technologies that aim at the elimination of toxic metal ions include e.g. the production of metal-bearing toxic sludge or other wastes requiring further handling, the need of additional chemicals and energy, the lack of selectivity and the often high costs [4, 5, 9].

Novel approaches, either for the analysis or removal of heavy metal ions, are based on the use of natural systems [5]. Several reviews discuss the high potentials of bioremediation in toxic metal ion removal from a contaminated area. These methods apply either passive metal ion uptake by dead biomass [3, 4, 9–12], the accumulation by living cells of microorganisms [9, 11–15], or the use of immobilized biomolecules [5, 16]. Adsorption, ion exchange, chelation by small molecules, micro-precipitation or binding to oligopeptides/proteins may operate in the sorption/accumulation mechanisms [9, 11]. The latter is certainly one of the most if not the most important interactions in the dynamic metal uptake pathway of microorganisms. As a consequence, genetically engineered bacteria overexpressing specific metal binding proteins [15] (e.g. metalloregulatory proteins [17] or metallothioneins [18]) or pre-designed oligopeptides fused to carrier proteins [14, 15, 19–23] may be promising candidates in metal ion removal. Appropriate peptides [6, 24–26] or the highly efficient and selective bacterial metal responsive metalloregulatory proteins [27] are also utilized in the construction of biosensors [7, 8, 28–30] for the detection of toxic metal ions. The applied sequences generally contain cysteines with a soft sulfur donor atom showing high affinity

towards the heavy metal ions. However, these can also bind zinc(II) being an essential micro-nutrient for bacteria.

In the present work we investigated the zinc(II)-binding of a novel 12-mer oligopeptide inspired by the metal binding domain of a CueR (Cu^+-efflux regulator) protein belonging to the MerR family of metalloregulators [31]. The ligand (Scheme 1) contains two cysteine residues as the most potent binding sites for d^{10} metal ions close to the termini of the molecule..In order to increase the flexibility of the ligand one of the two proline units of the native sequence was replaced by a serine residue that is, indeed, present in a number of other MerR family member proteins [31] being sensitive for divalent metal ions. The metal-bound peptide may form a loop structure, as shown previously for the cadmium(II)-complexes of a related ligand [32]. It may be asked, however, whether zinc(II) and cadmium(II) or mercury(II) form similarly stable and structurally analogous complexes with the dodecapeptide. As the zinc(II) level may exceed those of either cadmium(II) or mercury(II) in potential target media, selectivity of the binding would be essential for practical applications. Therefore, we also studied the possible competition of zinc(II) with cadmium(II) or mercury(II) in binding to the dodecapeptide.

2. Experimental

2.1. Materials

The investigated peptide *N-acetyl-Ser-Cys-Pro-Gly-Asp-Gln-Gly-Ser-Asp-Cys-Ser-Ile-NH_2 (Ac-SCPGDQGSDCSI-NH_2,* ***PS)*** was prepared by solid phase peptide synthesis using the Fmoc methodology (Fmoc = 9-fluorenylmethoxycarbonyl) and purified by reversed-phase HPLC, as described for a related ligand [32]. All other chemicals and solvents were obtained from Sigma-Aldrich and used without further purification unless otherwise described. Precisely weighed high purity $HgCl_2$ was used to prepare solutions with known $HgCl_2$

concentrations. Metal ion stock solutions prepared from $Zn(ClO_4)_2 \times 6H_2O$ and $CdCl_2 \times xH_2O$ were standardized complexometrically. pH-metric titrations were performed by NaOH (Aldrich) standard solution.

2.2. pH-potentiometric measurements

The protonation and complex formation equilibria were investigated by potentiometric titrations in aqueous solution (I = 0.1 M $NaClO_4$, T = 298.0 ± 0.1 K). Argon atmosphere in the titration cell was maintained with a special care throughout the titrations to avoid the oxidation of the peptide. An automatic titration set including a PC controlled Dosimat 665 (Metrohm) autoburette and an Orion 710A precision digital pH-meter equipped with a Metrohm Micro pH glass electrode (125 mm) was used for the experiments. The electrode was calibrated in aqueous solution via the modified Nernst equation [33]:

$$E = E_0 + K \cdot \log[\mathrm{H^+}] + J_{\mathrm{H}} \cdot [\mathrm{H^+}] + \frac{J_{\mathrm{OH}} \cdot K_{\mathrm{w}}}{[\mathrm{H^+}]}$$

where J_H and J_{OH} are fitting parameters in acidic and alkaline media for the correction of experimental errors mainly due to the liquid junction and to the alkaline and acidic errors of the glass electrode; $K_w = 10^{-13.75}$ M^2 is the autoprotolysis constant of water [34]. The parameters were calculated by the non-linear least squares method.

The protonation and complex formation processes were characterized by the following general equilibrium process:

$$\mathrm{pM + qH + rL} \rightleftharpoons \mathrm{M_pH_qL_r}$$

$$\beta_{\mathrm{M_pH_qL_r}} = \frac{[\mathrm{M_pH_qL_r}]}{[\mathrm{M}]^{\mathrm{p}}[\mathrm{H}]^{\mathrm{q}}[\mathrm{L}]^{\mathrm{r}}}$$

where M denotes the metal ion, L the non-protonated ligand molecule, and H the protons. Charges are omitted for simplicity, but can be easily calculated taking into account the composition of the fully protonated dodecapeptide (H_4L). The corresponding formation

constants ($\beta_{MpHqLr} \equiv \beta_{pqr}$) were calculated using the PSEQUAD computer program [35]. The protonation constants were determined from 4 independent titrations (60-80 data points per titration) with a peptide concentration of 1.0×10^{-3} M. Different ratios of zinc(II) ions and the ligand, i.e. 0.5:1, 1:1 and 2:1, were applied in the titrations of the zinc(II) – peptide system. We could observe foam formation at the surface of the solutions and slight precipitate formation was also visible in the presence of metal ion excess above neutral pH. Under these conditions no sign of dinuclear complex formation was seen in the ^{1}H NMR spectra. Accordingly, pH-potentiometric titrations with metal ion excess were not evaluated,. The complex formation constants were calculated from the remaining 4 titrations (60-80 data points per titration) where the applied ratio of zinc(II) and the ligand was 0.5:1 and 1:1 with the metal ion concentration varied between 4.0×10^{-4} and 1.0×10^{-3} M.

2.3. Electronic absorption and SRCD measurements

UV–visible (UV–Vis) spectra were measured on a UNICAM HELIOSα spectrophotometer using a cell with 0.5 cm optical pathlength equipped with a Teflon cap. Concentration of the ligand was 2.0×10^{-4} M and the metal ion concentration varied between 1.0×10^{-4} and 2×10^{-4} M, depending on the metal-to-ligand ratio. Spectra were measured in the 200-400 nm wavelength range. Samples were prepared under argon atmosphere and the optical cell was also filled with argon above the solution.

The synchrotron radiation CD (SRCD) spectra of the free ligand and the metal complexes were recorded at the SRCD facility at the CD1 beamline [36] on the storage ring ASTRID at the Institute for Storage Ring Facilities (ISA), University of Aarhus, Denmark. Camphor-sulfonic acid served as a calibration material for the instrument. All spectra were recorded with 1 nm steps and a dwell time of 2 s per step, using 0.1 mm quartz cells (SUPRASIL, Hellma GmbH, Germany), for the wavelength range of 170-330 nm. The

substances were initially dissolved in 1.0×10^{-2} M HCl in order to avoid the eventual oxidation process. The pH of the solutions of 1.0×10^{-3} M peptide concentration was adjusted by adding the appropriate amount of NaOH solution. For metal ion competition experiments different volumes of $CdCl_2$ or $HgCl_2$ stock solutions were added to the samples containing zinc(II) and **PS** in 1:1 molar ratio at pH ~ 6.5 to achieve a 0.33:1, 0.66:1, 1:1 and 2:1 molar ratio of the concentrations of the added metal ion and zinc(II), respectively. From raw spectra the water baseline was subtracted and spectra were normalized to a 1.0×10^{-3} M peptide concentration (to eliminate the effect of dilution).

2.4. NMR experiments

NMR measurements were performed on a Bruker Avance DRX 500 spectrometer operating at 500.13 MHz for ^{1}H. The spectra were recorded at T = 298 K in a mixture of H_2O/D_2O = 90:10 %v/v. In a typical sample the concentration of the peptide was 1.0×10^{-3} M. The pH of the samples was adjusted by NaOH solution. For the preparation of solutions containing cadmium(II) or mercury(II) ions besides zinc(II) calculated volumes of $CdCl_2$ or $HgCl_2$ stock solutions were added to the samples containing zinc(II) and **PS** in 1:1 molar ratio to achieve the desired molar ratio of the metal ion concentrations. The chemical shifts were calibrated to TSP (Trimethylsilyl propionate) as an external reference at 0.0 ppm (trimethylsilyl group). 1D ^{1}H NMR spectra were recorded using the zgpr pulse sequence with presaturation to reduce the H_2O/HDO resonances. All the spectra were recorded using a spectral width of 5 kHz and 128 scans.

Data were processed by the ACD/NMR Processor Academic Edition software [37].

2.5. Mass spectrometry

Mass spectrometry was performed on a Waters Micromass(R) Q-TOF Premier mass spectrometer operating in negative mode using electrospray ionization (ESI) source. In the samples the concentration of the peptide and those of the metal ions were 1.0×10^{-4} M and the pH of the solutions were set by ammonium hydrogen carbonate buffer (c = 10 mM) to pH = 7.6. The samples were transferred into the mass spectrometer by direct infusion at a flow rate of 5 μl/min. For better ionization methanol was infused at a flow rate of 5 μl/min via static mixing tee. The capillary and cone voltages were set to (+) 3.0 kV and (+) 25 V. The desolvation temperature was set to 150 ^{o}C and the source temperature to 80 ^{o}C. The cone gas was at a flow rate of 60 L/h, whereas the desolvation gas flow was maintained at 500 L/h. For qualitative analysis the identified zinc(II) and cadmium(II) complex ions were detected in an MS survey scan of 1 s from an m/z of 50 to 1990 using 5 eV collision energy. The MS was calibrated on a daily basis using sodium-formate solution in negative mode. All data were acquired and the theoretical isotope patterns were determined by MassLynx Mass Spectrometry Software V4.1 (Waters Inc.).

3. Results and Discussion

3.1. Speciation analysis of the zinc(II) - peptide system

The formation constants (logβ) determined for the proton and zinc(II) complexes are summarized in Table 1, together with some representative pKa values and derived stability data.

The ligand possesses four donor groups that undergo protonation/deprotonation processes in the studied pH-range (pH ~ 2–10.5). The release of two protons from the aspartic acid residues takes place between pH ~ 3–5 while overlapping deprotonations of the two cysteines can be detected between pH ~ 8–9.5.

Species distribution determined for the equimolar solution of zinc(II) and **PS** is presented in Fig. 1.A. Complex formation starts at pH ~ 4 and the appearance of ZnHL is immediately followed by the parent complex ZnL where all the dissociable protons of the ligand are released. The pK_a value for the process ZnHL $\rightarrow$ ZnL + H (= 5.02, see Table 1) is several log units lower compared to the pK_a values of the two cysteines of the free ligand (pK_{Cys} = 9.09 and 8.30) which strongly suggests the binding of both Cys-thiolates to zinc(II) in the ZnL complex. The determined stability of this species (log$K$ = 9.93) is somewhat higher than those of shorter peptides containing a CXC [38] or a longer ligand with a CASC motif [39], but lower compared to the stabilities formed with the Ac-CC-OH dipeptide [40] or longer peptides also containing neighboring cysteines and additional histidines in their sequences [41]. Even though the authors do not mention this possibility, in our view, the histidine residues may have a notable influence on the stability of the formed complexes (by metal ion coordination) which is very likely a stronger effect than that exerted by the aspartate units found in **PS** or in the ligand with a CASC sequence. This seems to be supported also by the significant differences between the stabilities determined for the three ligands containing the histidine residues in the peptide chain at different positions relative to the CC motif (Table 2) [41]. All in all, the comparison of the stability constants of the mono-complexes formed with various peptides reflect a relatively high affinity of **PS** to zinc(II) in spite the long distance between the Cys units and the formation of a macrochelate.

Further deprotonations occur above pH ~ 8 leading to the species $ZnH_{-1}L$ and $ZnH_{-2}L$ (Fig. 1.A). Since formation of hydroxide precipitates or the deprotonation of coordinated water ligands are well known phenomena of zinc(II) peptide complexes at alkaline pH [42, 43], in the absence of other potential deprotonating groups in **PS**, $ZnH_{-1}L$ and $ZnH_{-2}L$ are most probably hydroxo mixed ligand complexes and their compositions are better described as Zn(OH)L and $Zn(OH)_2L$, respectively.

The mono-complexes ZnHL and ZnL dominate in the acidic/neutral pH-range when **PS** is applied in a twofold excess over zinc(II) (Fig. 1.B). Bis-ligand complexes $ZnHL_2$ and ZnL_2 start to form above pH ~ 6 and ZnL_2 reaches a concentration maximum at ca. pH 9.4 (Fig. 1.B). Nevertheless, mono-complexes are present in significant amounts even in the range where bis-ligand species dominate and under basic conditions the second ligand starts to be released from metal ion coordination (Fig. 1.B). The stability constant calculated for the binding of the second ligand ($\log K_2 = 4.79$) is several log units smaller than $\log K_1$ (see Table 1) suggesting a relatively weak binding of the second coordinated **PS** within the parent bis-complex. The overall stability is also substantially lower than those of some di-, tri- or tetrapeptides (Table 2) [41, 44]. It is not surprising if one takes into account the size of the ligand and the fact that the thiolate residues are relatively far from each other in the peptide chain which may cause a steric hindrance for the binding of the second molecule. No bis-complex formation was suggested between zinc(II) and oligopeptides having two cysteine residues and similar size to that of **PS** [41]. However, as speculated above, histidine residues may participate in the binding of these ligands to zinc(II) that can stabilize mono-complexes and prevent the coordination of a second molecule. Additionally, the literature data are also somewhat incoherent regarding shorter peptides, since there has been opposite suggestions considering the existence of bis-complexes with tri- and tetrapeptides (see Refs. [38, 44] and data in Table 2). The fit of the potentiometric titration data of the zinc(II) – **PS** 0.5:1 system with a model containing no bis-complexes resulted in a significant deviation between the experimental and fitted curves (Fig. S1) and a three-fold higher fitting parameter as compared to the accepted model. This clearly suggests that under the conditions of our studies a second **PS** molecule, although with a relatively weak binding strength, coordinates to zinc(II).

3.2. Spectroscopic studies on the zinc(II) - peptide complexes

The coordination mode of the ligand within the complexes formed between zinc(II) and **PS** were investigated by UV, SRCD (synchrotron radiation circular dichroism) and ^{1}H NMR spectroscopies.

UV spectra were recorded as a function of pH both in the equimolar solution of the metal ion and ligand and in the presence of twofold ligand excess. Coordination of deprotonated thiol groups to zinc(II) results in a $-S^- \rightarrow Zn^{2+}$ LMCT band around 230 nm as it was shown for zinc(II)-metallothioneins [45, 46]. Such electron transitions have also been observed for the zinc(II) complexes of several cysteine containing oligopeptides [47–51]. pH-dependent absorbance increase was found in the wavelength range of 220 – 270 nm during the titration of samples containing zinc(II) and **PS** in 1:1 and 0.5:1 ratios (Figs. S2.A-B). The measured absorbances at 235 nm are compared to the distribution of complex species on Fig. 1.A and B. The absorbance starts to increase from pH ~ 4, in parallel with the coordination of zinc(II) to the peptide. In the presence of one equivalent metal ion per ligand the observed steep absorbance change and the plateau on the curve between pH ~ 6.5–8 is clearly related to the formation of the ZnL complex, strongly suggesting the binding of both Cys-thiolate groups to the metal ion. Further increase of the absorbance values at higher pH can be attributed to the formation of Zn(OH)L and $Zn(OH)_2L$ that might cause rearrangement in the coordination sphere of zinc(II) and a change of electron density on the metal ion center. At twofold excess of **PS** over zinc(II) a narrow break in the increase of absorbances can be observed between pH ~ 6–7.5 which is in a rather good correlation with the species distribution curves showing the maximum abundance of the parent mono-complex ZnL in the same pH-range. Above pH ~ 8 the A_{235nm} vs. pH curve seems to follow the formation of bis-complexes. It has to be noted, however, that deprotonated thiol groups also possess a relatively intense absorption around λ = 236 nm assigned to an $n \rightarrow \sigma^*$ transition [52]. Since the suggested bis-complex formation and deprotonation of the Cys residues of free **PS** take

place in a similar pH-range, the observed increase of absorbance above pH ~ 8 is very likely the result of parallel processes. The species distribution calculated from the determined stability constants (Table 1) for the concentrations applied in the UV experiments demonstrate, that the binding of additional thiolate groups of a second **PS** molecule to the zinc(II) center, and deprotonation of the thiol groups of the free **PS** or unbound cysteine residues of the ligand all contribute to the observed UV absorbance change in the alkaline pH-range.

The pH-dependent series of ^{1}H NMR spectra recorded in the zinc(II) – **PS** 1:1 system (Fig. 2) correlate well with the information provided by pH-potentiometric and UV data. The spectrum measured at pH = 4.65 is very similar to that of the free ligand at the same pH (see Fig. S3) suggesting that the major fraction of **PS** is not coordinated to the metal ion. The increase of pH results in a significant line broadening of most of the resonances referring to an intermediate exchange rate, relative to the NMR time scale, between species, i.e. complexed and unbound **PS** molecules. Signals become sharp at neutral pH where practically all the ligands are bound to zinc(II) in a form of ZnL. Under basic conditions the spectrum becomes less resolved again as several exchanging species co-exist.

SRCD spectra reflect the change of peptide conformation and thus may provide valuable information on the complex formation processes and complex structures, but from a different approach, as compared to ^{1}H NMR spectra. The SRCD spectra of **PS**, even in the presence of zinc(II) resembles random coil like signatures of disordered protein structures, represented by a minimum around 197-200 nm and a weak shoulder around 220 nm (see Fig. 3) [53, 54]. Spectra measured in the absence and presence of zinc(II) at pH = 3 are almost identical indicating no complex formation at this pH (spectra not shown). A significant decrease of ellipticity between 210-230 nm can be observed at pH = 6.5 (Fig. 3) in line with the formation of ZnL with two bound cysteine thiolates of **PS**. Similar type, but even more

pronounced change has been observed for a phytochelatin analogue ((Glu–Cys)$_4$–Gly) in the presence of zinc(II) [50]. The relatively small deviation of the spectrum attributed to ZnL from that of free **PS** may suggest that the peptide backbone still has a lot of conformational flexibility in the bound form. Formation of dimeric Zn_2L_2 species with zinc(II) ions bridging the two ligands through the thiolate moieties, however, cannot be ruled out. At alkaline pH, where the formation of hydroxo mixed ligand complexes are indicated by potentiometric titrations, the structure of **PS** changes further, as demonstrated by the slight red shift of the CD-intensity minimum and the collapse of the shoulder at 220 nm (Fig. 3).

Fig. 4 shows a series of ^{1}H NMR spectra recorded at selected pH values with varying zinc(II) – peptide ratio around neutral pH focusing on the resonances being the most affected by the metal ion – ligand interaction, i.e. the signals of $C_\beta H_2$ protons of the Cys and Asp residues. In the presence of ligand excess (spectrum 'b' in Fig. 4) all the observed signals are significantly broadened, similarly to what was seen at pH = 5.62 at 1:1 ratio of zinc(II) and **PS** (see Fig. 2). Species distribution curves reveal the presence of ca. 35 % of the total zinc(II) in bis-ligand complexes, which means that at least 3 species (ZnL, ZnH_2L and unbound **PS**) co-exist with an intermediate ligand exchange between them. Concerning bis-complex formation, spectra measured at higher pH could be obviously more informative, however, even at higher pH one would see the influence of co-existing species on the shape of spectra. Furthermore, at higher pH we faced the problem that the oxidation of the ligand became a much more rapid process along with the deprotonation of thiol groups.

At 1:1 ratio of zinc(II) and **PS** (spectrum 'c' in Fig. 4) the observed signals are well resolved and the splitting patterns of the ^{2,10}Cys $C_\beta H_2$ resonances remarkably differ from those of the same resonances of the free ligand (spectrum'a' in Fig. 4). This, similarly to all the other experiments discussed so far, reflects thiolate binding to zinc(II). Although Cys and Asp related signals strongly overlap, it is clear, that the ^{5,9}Asp $C_\beta H_2$ resonances are also

significantly changed. They spread over a broader ppm range in comparison to the unbound ligand signals, i.e. a set of resonances, presumably belonging to one of the Asp residues is notably shifted downfield. Downfield shift of the $C_\beta H_2$ resonances of an aspartic acid residue of a similar peptide has been attributed to carboxylate binding to cadmium(II) ion [32]. These findings suggest binding of one of the carboxylate side chains of **PS** to zinc(II), besides the two thiolates.

The excess of zinc(II) ions over **PS** cause no change at any region of the ^{1}H NMR spectrum as compared to the one recorded at 1:1 ratio (see spectrum 'd' in Fig. 4). This stands also for the spectra measured at lower or higher pH values, which undoubtedly suggests that dinuclear species are not formed even in the presence of metal ion excess. Indeed, around pH 9, white precipitate appeared in the samples containing twofold zinc(II) excess over **PS** due to the hydrolysis of free zinc(II) ions. On the other hand it has to be noted that in the cadmium(II) – **PS** or mercury(II) – **PS** systems the second metal ions apparently binds to the ligand (see later).

*3.3. Competition of zinc(II) with cadmium(II) or mercury(II) in binding to **PS***

Competition of the d^{10} metal ions in binding to the ligand **PS** was studied around neutral pH by means of SRCD and ^{1}H NMR experiments. The question to be answered was: how the presence of zinc(II) ions might influence the binding of the oligopeptide to the toxic metal ions, cadmium(II) or mercury(II). Transition metal ions have typical preferences for certain type of donor ligands, but also for coordination geometries [55]. In proteins and peptides, mercury(II) is known to have an outstanding affinity for the soft sulfur ligands and a strong preference for linear [56–59] or trigonal coordination geometries [59–62], however, it can also adopt a tetrahedral coordination environment of donor groups [63–65]. In contrast, cadmium(II) and zinc(II) prefer tetrahedral coordination geometry [55, 59, 65], but higher

coordination numbers are also easily possible, especially for the more flexible zinc(II) ions [55, 66]. The binding affinities of d^{10} metal ions to cysteine follow the order of $Hg^{2+} > Cd^{2+} > Zn^{2+}$ [67, 68] which usually also stands for metallothioneins [67] and MerR metalloregulatory proteins [68]. Considering the known ligand and geometry preferences of the three metal ions, **PS** is expected to have a higher affinity towards mercury(II), as compared to cadmium(II) or zinc(II). Nevertheless, metal ion affinities, especially within proteins, are influenced by several factors, and general predictions are not always possible [69]. It is nicely demonstrated by the almost identical dissociation constant of zinc(II) and cadmium(II) with the $(Cys)_4$ zinc-finger binding site of the Estrogen receptor DNA-binding domain [70].

SRCD titration of the zinc(II) – **PS** 1:1 system with cadmium(II) ions resulted in a continuous change of the spectra up to the 1:1:1 zinc(II):**PS**:cadmium(II) concentration ratio, suggesting the binding of cadmium(II) ions to the ligand and the release of zinc(II) (Fig. 5). However, the spectrum obtained in the presence of one equivalent cadmium(II) slightly differs from that of the cadmium(II) – **PS** 1:1 system recorded at the same pH. ^{1}H NMR titrations performed with the same series of samples also around neutral pH reflects the same process (Fig. 6), nevertheless the difference between the ^{1}H NMR spectra of the ternary system (spectrum 'b' in Fig. 6) and the sample containing cadmium(II) and ligand in a 1:1 ratio (spectrum'd' in Fig. 6) is much more pronounced. This may originate from the presence of zinc(II) complexes even when one equivalent of cadmium(II) is added, which would imply comparable affinities of **PS** towards the two metal ions. However, the previously observed stabilities of zinc(II) and cadmium(II) complexes of some two Cys-containing short peptides, point to a ca. two orders of magnitude stronger affinity of the ligands in cadmium(II) binding [39, 41]. On the other hand, one should not exclude the possibility of the presence of heterodinuclear complexes in some extent, i.e. species where zinc(II) is also bound to the ligand besides cadmium(II). Although no specific structures for such species can be proposed

from our data, mixed binding of zinc(II) and other metal ions (including cadmium(II) and mercury(II)) to certain zinc finger sites has already been suggested [65, 69, 71, 72].

ESI-MS spectra were also recorded to search for additional support for either of the above assumptions. As demonstrated in Fig. 7, isotope pattern representing a zinc(II) containing monomeric double charged species, i.e. $[ZnL]^{2-}$ as a minor component was also observable together with the isotope pattern of $[CdL]^{2-}$ being the most abundant ion in the solution containing zinc(II), **PS** and cadmium(II) in a 1:1:1 ratio. Not surprisingly, $[ZnL]^{2-}$ proved to be the most abundant ion in the sprayed sample of the equimolar solution of zinc(II) and the ligand. No signals representing ternary species of either dinuclear or dimeric type have been detected under the conditions of the MS experiments, which is of course not a conclusive proof against the presence of such complexes. Nevertheless, the information provided by the MS spectra nicely correlate with the other spectroscopic data representing the partial replacement of zinc(II) by cadmium(II) at the binding sites of **PS** when the three components are present in 1:1:1 concentration ratio.

The addition of another equivalent of cadmium(II) to the titrated samples resulted in remarkable changes both on the SRCD (Fig. 5) and ^{1}H NMR spectra (Fig. 6). More importantly, these spectra are almost identical to those recorded in the solutions containing only cadmium(II) and **PS** in a 2:1 ratio. This undoubtedly points to the formation of dinuclear cadmium(II) complexes, but also reflects the complete replacement of zinc(II) from the binding sites of the ligand. (Equilibrium and solution structural investigation of the cadmium(II) and mercury(II) complexes of the peptide will be published later.)

When mercury(II) is added gradually to the zinc(II) – **PS** 1:1 system the intensity of the CD-minimum around 198 nm decreases while the small negative ellipticity around 220 nm increases (Fig. 8). The observed SRCD spectrum in the presence of one equivalent of mercury(II) besides zinc(II) and **PS** is very close to the one measured for the mercury(II) – **PS**

1:1 binary system. A perfect match of ^{1}H NMR spectra for these two samples can be observed, too (see spectra ‘b’ and ‘d’ on Fig. 9). Mercury(II), when present in an even concentration compared to zinc(II) and **PS**, can fully replace the less soft zinc(II) ion from the binding sites of the ligand.

A significant change occurs on the SRCD spectra when adding the second equivalent of mercury(II) to the sample (Fig. 8). The ellipticity around 198 nm is collapsed while the lower energy shoulder is shifted to $\lambda \sim 230$ nm. Surprisingly, the observed spectrum is distinct from the one measured for the mercury(II) – **PS** 2:1 binary system. At the same time, ^{1}H NMR spectra obtained for the samples of mercury(II) – **PS** with a 2:1 ratio in the presence and absence of zinc(II) look similar, but not exactly the same. Nevertheless, they are less informative due to the observed strong line broadening (spectra ‘c’ and ‘e’ on Fig. 9). We assume, that coordination of the second mercury(II) ion to the peptide breaks the loop-type coordination mode of the ligand adopted in the mono-complexes of either zinc(II) or mercury(II) and this conformational change makes the carboxylate groups of the ligand more available for weak zinc(II)-binding.

According to these data, mercury(II) fully replaces zinc(II) from the thiolate binding sites of **PS** up to a 1:1 ratio of the metal ions, nevertheless, excess of mercury(II) results in a significantly altered ligand conformation likely to provide better access to the carboxylate moieties for other metal ions, including zinc(II).

4. Conclusion

The investigated dodecapeptide, possessing two cysteine and two aspartate residues as potential metal binding sites, binds zinc(II) ions with a remarkably high affinity and forms differently protonated mono- and bis-complexes from pH ~ 4. Besides the coordination of the deprotonated thiol groups participation of one of the Asp-carboxylates is suggested in the ZnL

parent complex. Competition studies on the binding of zinc(II) and cadmium(II) or zinc(II) and mercury(II) ions to the ligand showed that zinc(II) cannot prevent the coordination of toxic metal ions to the thiolate donor groups of the ligand. However, while one equivalent of mercury(II) fully replaces zinc(II) from its mono-complex, formation of mixed metal ion complexes is also presumable besides zinc(II)-replacement, in case of cadmium(II). Nevertheless, excess of cadmium(II) over zinc(II) leads to the formation of dinuclear species and the complete release of zinc(II) from the peptide.

Based on our findings the investigated dodecapeptide can be considered as a promising candidate for toxic metal ion binding in practical applications, especially, for mercury(II) ions.

5. Abbreviations

Ac-SCPGDQGSDCSI-NH_2 (**PS**): N-acetyl-Ser-Cys-Pro-Gly-Asp-Gln-Gly-Ser-Asp-Cys-Ser-Ile-NH_2

MerR: a family of transcriptional regulators the archetype of which is the Hg^{2+}-responsive transcriptional repressor-activator MerR protein

CueR: Cu^{+}-efflux regulator protein

SRCD: synchrotron radiation circular dichroism

ESI source: electrospray ionization source

LMCT: ligand-to-metal charge transfer

Acknowledgements

The authors kindly acknowledge the financial support of the project by the European Union's European Regional Development Fund, provided within the frameworks of the Hungary-Romania Cross-Border Cooperation Programme 2007-2013 under project No.

HURO/1001/232/2.2.2. (METCAP). AJ wishes to thank the financial support of the János Bolyai Research Grant from the Hungarian Academy of Sciences. The research leading to the SRCD results has received funding from the European Community's Seventh Framework Programme (FP7/2007-2013) under grant agreement Nº 226716.

Supplementary data

Supplementary material associated with this article can be found:

References

[1] J. Nriagu, J. Pacyna, Nature 333 (1988) 134–139.

[2] R.S. Boyd, J. Chem. Ecol. 36 (2010) 46–58.

[3] B. Volesky, Z.R. Holan, Biotechnol. Prog. 11 (1995) 235–50.

[4] B. Volesky, Hydrometallurgy 59 (2001) 203–216.

[5] L. Malachowski, J. Stair, Pure Appl. Chem. 76 (2004) 777–787.

[6] H. Satofuka, S. Amano, H. Atomi, M. Takagi, K. Hirata, K. Miyamoto, T. Imanaka, J. Biosci. Bioeng. 88 (1999) 287–92.

[7] I. Bontidean, E. Csöregi, P. Corbisier, J.R. Lloyd, N.L. Brown, in: Heavy Metals in the Environment, Marcel Dekker, New York, 2002, pp. 647–680.

[8] N. Verma, M. Singh, BioMetals 18 (2005) 121–129.

[9] A.I. Zouboulis, M.X. Loukidou, K.A. Matis, Process Biochem. 39 (2004) 909–916.

[10] G.M. Gadd, C. White, Trends Biotechnol. 11 (1993) 353–9.

[11] J. Wang, C. Chen, Biotechnol. Adv. 27 (2009) 195–226.

[12] M. Valls, V. de Lorenzo, FEMS Microbiol. Rev. 26 (2002) 327–38.

[13] J.R. Lloyd, D.R. Lovley, Curr. Opin. Biotechnol. 12 (2001) 248–53.

[14] W. Bae, W. Chen, A. Mulchandani, R.K. Mehra, Biotechnol. Bioeng. 70 (2000) 518–24.

[15] M. Mejáre, L. Bülow, Trends Biotechnol. 19 (2001) 67–73.

[16] J.L. Stair, J.A. Holcombe, Microchem. J. 81 (2005) 69–80.

[17] W. Bae, C.H. Wu, J. Kostal, A. Mulchandani, W. Chen, Appl. Environ. Microbiol. 69 (2003) 3176–3180.

[18] S. Sauge-Merle, C. Lecomte-Pradines, P. Carrier, S. Cuiné, M. Dubow, Chemosphere 88 (2012) 918–24.

[19] P. Kotrba, L. Dolecková, V. de Lorenzo, T. Ruml, Appl. Environ. Microbiol. 65 (1999) 1092–8.

[20] A. Bouia, A. Kholti, M. Saghi, P. Cornelis, Res. Microbiol. 152 (2001) 799–804.

[21] C.-C. Huang, C.-C. Su, J.-L. Hsieh, C.-P. Tseng, P.-J. Lin, J.-S. Chang, Enzyme Microb. Technol. 33 (2003) 379–385.

[22] J. Qin, L. Song, H. Brim, M.J. Daly, A.O. Summers, Microbiology (Reading, Engl.) 152 (2006) 709–19.

[23] S. Vinopal, T. Ruml, P. Kotrba, Int. Biodeter. Biodegr. 60 (2007) 96–102.

[24] I. Bontidean, J. Ahlqvist, A. Mulchandani, W. Chen, W. Bae, R.K. Mehra, A. Mortari, E. Csöregi, Biosens. Bioelectron. 18 (2003) 547–553.

[25] B.R. White, J.A. Holcombe, Talanta 71 (2007) 2015–20.

[26] B.P. Joshi, K.-H. Lee, Bioorg. Med. Chem. 16 (2008) 8501–9.

[27] Z. Ma, F.E. Jacobsen, D.P. Giedroc, Chem. Rev. 109 (2009) 4644–4681.

[28] I. Bontidean, J.R. Lloyd, J.L. Hobman, J.R. Wilson, E. Csöregi, B. Mattiasson, N.L. Brown, J. Inorg. Biochem. 79 (2000) 225–9.

[29] P. Chen, C. He, J. Am. Chem. Soc. 126 (2004) 728–729.

[30] S. V Wegner, A. Okesli, P. Chen, C. He, J. Am. Chem. Soc. 129 (2007) 3474–5.

[31] A. Changela, K. Chen, Y. Xue, J. Holschen, C.E. Outten, T. V O'Halloran, A. Mondragón, Science 301 (2003) 1383–7.

[32] A. Jancsó, D. Szunyogh, F.H. Larsen, P.W. Thulstrup, N.J. Christensen, B. Gyurcsik, L. Hemmingsen, Metallomics 3 (2011) 1331–9.

[33] F.J.C. Rosotti, H. Rosotti, *The Determination of Stability Constants*, McGraw-Hill Book Co., New York, 1962.

[34] E. Högfeldt, *Stability Constants of Metal-Ion Complexes, Part A. Inorganic Ligands*, Pergamon, New York, 1982.

[35] L. Zékány, I. Nagypál, G. Peintler, *PSEQUAD for Chemical Equilibria*, Technical Software Distributors, Baltimore, MD, 1991.

[36] P. Limão-Vieira, A. Giuliani, J. Delwiche, R. Parafita, R. Mota, D. Duflot, J.-P. Flament, E. Drage, P. Cahillane, N.J. Mason, S.V. Hoffmann, M.-J. Hubin-Franskin, Chem. Phys. 324 (2006) 339–349.

[37] *ACD/NMR Processor Academic Edition, version 12.01*, Advanced Chemistry Development, Inc., Toronto, ON, Canada, www.acdlabs.com, 2010.

[38] P. Gockel, M. Gelinsky, R. Vogler, H. Vahrenkamp, Inorg. Chim. Acta 272 (1998) 115–124.

[39] K. Krzywoszynska, M. Rowinska-Zyrek, D. Witkowska, S. Potocki, M. Luczkowski, H. Kozlowski, Dalton Trans. 40 (2011) 10434–10439.

[40] R. Vogler, M. Gelinsky, L.F. Guo, H. Vahrenkamp, Inorg. Chim. Acta 339 (2002) 1–8.

[41] M. Rowinska-Zyrek, D. Witkowska, S. Bielinska, W. Kamysz, H. Kozlowski, Dalton Trans. 40 (2011) 5604–10.

[42] I. Sóvágó, K. Ősz, Dalton Trans. (2006) 3841–54.

[43] I.N. Jakab, O. Lőrincz, A. Jancsó, T. Gajda, B. Gyurcsik, Dalton Trans. (2008) 6987–95.

[44] K. Kulon, D. Woźniak, K. Wegner, Z. Grzonka, H. Kozłowski, J. Inorg. Biochem. 101 (2007) 1699–706.

[45] M. Vasak, J.H.R. Kaegi, H.A.O. Hill, Biochemistry 20 (1981) 2852–2856.

[46] J.H. Kägi, M. Vasák, K. Lerch, D.E. Gilg, P. Hunziker, W.R. Bernhard, M. Good, Environ. Health Perspect. 54 (1984) 93–103.

[47] E.-D. Ciuculescu, Y. Mekmouche, P. Faller, Chem. Eur. J. 11 (2005) 903–9.

[48] T. Kochanczyk, P. Jakimowicz, A. Krezel, Chem. Commun. (2013).

[49] U. Heinz, M. Kiefer, A. Tholey, H.-W. Adolph, J. Biol. Chem. 280 (2005) 3197–207.

[50] Y. Cheng, Y.-B. Yan, J. Liu, J. Inorg. Biochem. 99 (2005) 1952–62.

[51] R. Kobayashi, E. Yoshimura, Biol. Trace Elem. Res. 114 (2006) 313–8.

[52] N.A. Rey, O.W. Howarth, E.C. Pereira-Maia, J. Inorg. Biochem. 98 (2004) 1151–9.

[53] S. Venyaminov, I. Baikalov, Z. Shen, C. Wu, T. Yang, Anal. Biochem. 214 (1993) 17–24.

[54] V. Uversky, Protein Sci. 11 (2002) 739–756.

[55] R.M. Roat-Malone, *Bioinorganic Chemistry: A Short Course*, Second Ed., John Wiley & Sons, Inc., Hoboken, NJ, USA, 2007.

[56] R.A. Steele, S.J. Opella, Biochemistry 36 (1997) 6885–95.

[57] G. Veglia, F. Porcelli, T. DeSilva, A. Prantner, S. Opella, J. Am. Chem. Soc. 122 (2000) 2389–2390.

[58] O. Sénèque, S. Crouzy, D. Boturyn, P. Dumy, M. Ferrand, P. Delangle, Chem. Commun. (2004) 770–1.

[59] T.T. Ngu, M.J. Stillman, IUBMB Life 61 (2009) 438–46.

[60] G.R. Dieckmann, D.K. McRorie, J.D. Lear, K. a Sharp, W.F. DeGrado, V.L. Pecoraro, J. Mol. Biol. 280 (1998) 897–912.

[61] X. Li, K. Suzuki, K. Kanaori, K. Tajima, A. Kashiwada, H. Hiroaki, D. Kohda, T. Tanaka, Protein Sci. 9 (2000) 1327–33.

[62] O. Iranzo, P.W. Thulstrup, S.-B. Ryu, L. Hemmingsen, V.L. Pecoraro, Chem. Eur. J. 13 (2007) 9178–90.

[63] P. Faller, B. Ctortecka, W. Tröger, T. Butz, M. Vasák, J. Biol. Inorg. Chem. 5 (2000) 393–401.

[64] M. Łuczkowski, M. Stachura, V. Schirf, B. Demeler, L. Hemmingsen, V.L. Pecoraro, Inorg. Chem., 47 (2008) 10875–88.

[65] U. Heinz, L. Hemmingsen, M. Kiefer, H.-W. Adolph, Chem. Eur. J. 15 (2009) 7350–8.

[66] Z. Paksi, A. Jancsó, F. Pacello, N. Nagy, A. Battistoni, T. Gajda, J. Inorg. Biochem. 102 (2008) 1700–10.

[67] K.B. Nielson, C.L. Atkin, D.R. Winge, J. Biol. Chem. 260 (1985) 5342–50.

[68] D.M. Ralston, T. V O'Halloran, Proc. Natl. Acad. Sci. U.S.A. 87 (1990) 3846–50.

[69] A. Hartwig, Antioxid. Redox Signaling 3 (2001) 625–634.

[70] P.F. Predki, B. Sarkar, J. Biol. Chem. 267 (1992) 5842–6.

[71] H. Thiesen, C. Bach, Biochem. Biophys. Res. Commun. 176 (1991) 551–557.

[72] M. Razmiafshari, N.H. Zawia, Toxicol. Appl. Pharmacol. 166 (2000) 1–12.

Table 1: Formation constants (logβ) of the proton and zinc(II) complexes of **PS** (with the estimated errors of the last digits in parentheses) together with derived data (I = 0.1 M $NaClO_4$, T = 298 K). Charges of the species are given in the table, but omitted throughout the text for simplicity.

Species	pqr	lgβ_{pqr}		pK_{ligand}
$[HL]^{3-}$	011	9.09(2)	p$K_{a,4}$	9.09
$[H_2L]^{2-}$	021	17.39(2)	p$K_{a,3}$	8.30
$[H_3L]^{-}$	031	21.76(2)	p$K_{a,2}$	4.37
H_4L	041	25.26(3)	p$K_{a,1}$	3.50
				pK_{pqr} [a], logK_2^{L} [b]
$[ZnHL]^{-}$	111	14.95(8)	pK_{111}	5.02
$[ZnL]^{2-}$	101	9.93(2)	pK_{101}	9.11
$[ZnH_{-1}L]^{3-}$	1–11	0.82(4)	pK_{1-11}	10.50
$[ZnH_{-2}L]^{4-}$	1–21	–9.68(4)		
$[ZnHL_2]^{5-}$	112	23.0(1)	pK_{112}	8.3
$[ZnL_2]^{6-}$	102	14.72(7)	lgK_2^{L}	4.79
FP (cm^3) [c]		0.002		

[a] $pK_{pqr} = \log \beta_{pqr} - \log \beta_{p(q-1)r}$; [b] $\log K_2^{L} = \log \beta_{102} - \log \beta_{101}$; [c] FP = fitting parameter

Table 2: Stability data of the zinc(II) complexes of selected terminally protected oligopeptides containing two cysteines

Ligand	$\log\beta_{ZnL}$	$\log\beta_{ZnL_2}$	$\log\beta_{H_2L}$	Ref.
Ac-CC-OH	11.0	21.8	18.94	[40]
Ac-CC-NH_2	–	17.63	17.31	[41]
Ac-CVC-NH_2	9.39	–	17.74	[38]
Ac-CPC-NH_2	9.31	–	17.85	[38]
Ac-CGC-NH_2	–	18.81	17.26	[44]
Ac-CPCP-NH_2	–	18.81	17.44	[44]
Ac-GSCCHTGNHD-NH_2	11.75	–	17.43	[41]
Ac-EEGCCHGHHE-NH_2	13.15	–	18.11	[41]
Ac-CCSTSDSHHQ-NH_2	10.90	–	17.28	[41]
Ac-SCPGDQGSDCSI-NH_2 (**PS**)	9.93	14.72	17.39	This work
Ac-GCASCDNARAAKK-NH_2	$\log\beta_{ZnHL}$ = 20.11 [a]		pK_{Lys} = 10.90	[39]

[a] Stability constant for ZnHL can be calculated by the equation: $\log K_{ZnHL} = \log\beta_{ZnHL} - \log\beta_{HL}$ = 20.11 – 10.90 = 9.21.

Captions for Schemes and Figures

Scheme 1.: Schematic structure of Ac-SCPGDQGSDCSI-NH_2 (**PS**)

Fig. 1: Species distribution diagram for zinc(II) : **PS** 1:1 (A), and 0.5:1 (B) systems (charges of the complex species are omitted for simplicity, $c_{\mathbf{PS}} = 1.0\times10^{-3}$ M, I = 0.1 M $NaClO_4$, T = 298 K). The squares represent the change of absorbance at 235 nm.

Fig. 2: Selected region of the ^{1}H NMR spectra of the peptide **PS** recorded in the zinc(II) – **PS** 1:1 system as a function of pH ($c_{\mathbf{PS}} = 1.0\times10^{-3}$ M, T = 298 K, 10 % w/w D_2O/H_2O). Signals from the ^{2,10}Cys $C_\beta H_2$ and ^{5,9}Asp $C_\beta H_2$ resonances (marked on the figure) and those of the ^{6}Gln $C_\gamma H_2$, ^{3}Pro $C_\beta H_2$, ^{6}Gln $C_\beta H_2$, CH_3CO-^{1}Ser, ^{3}Pro $C_\gamma H_2$ and ^{12}Ile $C_\beta H$ resonances (between $\delta \sim$ 2.5 – 1.8 ppm) are shown. Tentative assignment has been made based on the fully assigned resonances of a closely related dodecapeptide [32].

Fig. 3: SRCD spectra recorded in the zinc(II) – **PS** 1:1 system at different pH values: triangle, pH = 5.5; circle, pH = 6.5; square, pH = 10.0. As a comparison, spectrum of free **PS** at pH = 6.5 (dashed line with open circles) is also shown. ($c_{\mathbf{PS}} = 1.0\times10^{-3}$ M, T = 298 K)

Fig. 4: Selected region of the ^{1}H NMR spectra of the peptide **PS** recorded at pH ~ 7.6 as a function of the metal ion to peptide ratio: (a), free **PS** pH = 7.59; (b), 0.5 eq. Zn^{2+} + **PS** pH = 7.76; (c), 1 eq. Zn^{2+} + **PS** pH = 7.67; (d), 2 eq. Zn^{2+} + **PS** pH = 7.66. ($c_{\mathbf{PS}} = 1.0\times10^{-3}$ M, T = 298 K, 10 % w/w D_2O/H_2O).

Fig 5: SRCD titration of the zinc(II) – **PS** 1:1 system at pH = 6.5 with cadmium(II) (only the characteristic curves at 0, 1 and 2 equivalents of Cd^{2+} is shown) and comparison of spectra with those recorded in the cadmium(II) – **PS** 1:1 and 2:1 systems: circle, Zn^{2+}:**PS** 1:1; triangle, Zn^{2+}:**PS** 1:1 + 1 eq. Cd^{2+}; square, Zn^{2+}:**PS** 1:1 + 2 eq. Cd^{2+}; dashed line with open triangle, Cd^{2+}:**PS** 1:1; dashed line with open square, Cd^{2+}:**PS** 2:1. ($c_{\mathbf{PS}}$ = 1.0×10^{-3} M, T = 298 K)

Fig. 6: ^{1}H NMR titration of the zinc(II) – **PS** 1:1 system at pH ~ 7.6 with cadmium(II) and comparison of spectra with those recorded in the cadmium(II) – **PS** 1:1 and 2:1 systems: (a), Zn^{2+}:**PS** 1:1 pH = 7.65; (b) Zn^{2+}:**PS** 1:1 + 1 eq. Cd^{2+} pH = 7.62; (c), Zn^{2+}:**PS** 1:1 + 2 eq. Cd^{2+} pH = 7.63; (d), Cd^{2+}:**PS** 1:1 pH = 7.50; (e), Cd^{2+}:**PS** 2:1 pH = 8.06. ($c_{\mathbf{PS}}$ = 1.0×10^{-3} M, T = 298 K, 10 % w/w D_2O/H_2O)

Fig. 7: Theoretical isotope pattern of $[ZnL]^{2-}$ (at 634.171 monoisotopic m/z) (A), measured isotope pattern of $[ZnL]^{2-}$ (at 634.149 monoisotopic m/z) (B) and $[CdL]^{2-}$ (at 657.139 monoisotopic m/z) (C), and theoretical isotope pattern of $[CdL]^{2-}$ (at 657.159 monoisotopic m/z) (D). L represents the fully deprotonated –4 charged **PS** molecule.

Fig. 8: SRCD titration of the zinc(II) – **PS** 1:1 system with mercury(II) at pH = 6.5 (only the characteristic curves at 0, 1 and 2 equivalents of Hg^{2+} is shown) and comparison of spectra with those recorded in the mercury(II) – **PS** 1:1 and 2:1 systems: circle, Zn^{2+}:**PS** 1:1; triangle, Zn^{2+}:**PS** 1:1 + 1 eq. Hg^{2+}; square, Zn^{2+}:**PS** 1:1 + 2 eq. Hg^{2+}; dashed line with open triangle, Hg^{2+}:**PS** 1:1; dashed line with open square, Hg^{2+}:**PS** 2:1. ($c_{\mathbf{PS}}$ = 1.0×10^{-3} M, T = 298 K)

Fig. 9: ^{1}H NMR titration of the zinc(II) – **PS** 1:1 system at pH ~ 7.5 with mercury(II) and comparison of spectra with those recorded in the mercury(II) – **PS** 1:1 and 2:1 systems: (a), Zn^{2+}:**PS** 1:1 pH = 7.65; (b) Zn^{2+}:**PS** 1:1 + 1 eq. Hg^{2+} pH = 7.37; (c), Zn^{2+}:**PS** 1:1 + 2 eq. Hg^{2+} pH = 7.36; (d), Hg^{2+}:**PS** 1:1 pH = 7.08; (e), Hg^{2+}:**PS** 2:1 pH = 7.23. ($c_{\mathbf{PS}} = 1.0\times10^{-3}$ M, T = 298 K, 10 % w/w D_2O/H_2O)

Scheme_1

Click here to download high resolution image

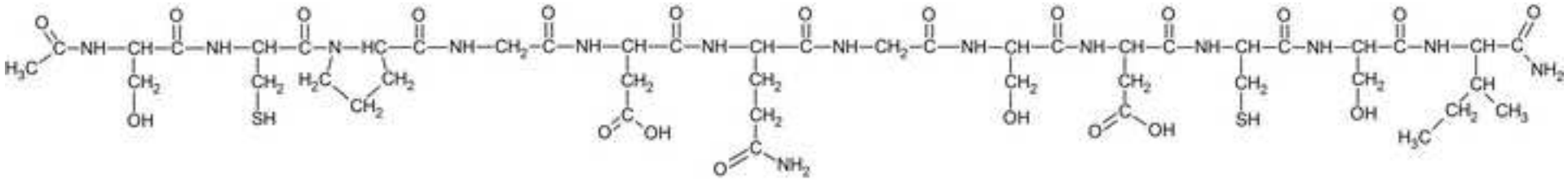

Fig_1

Click here to download high resolution image

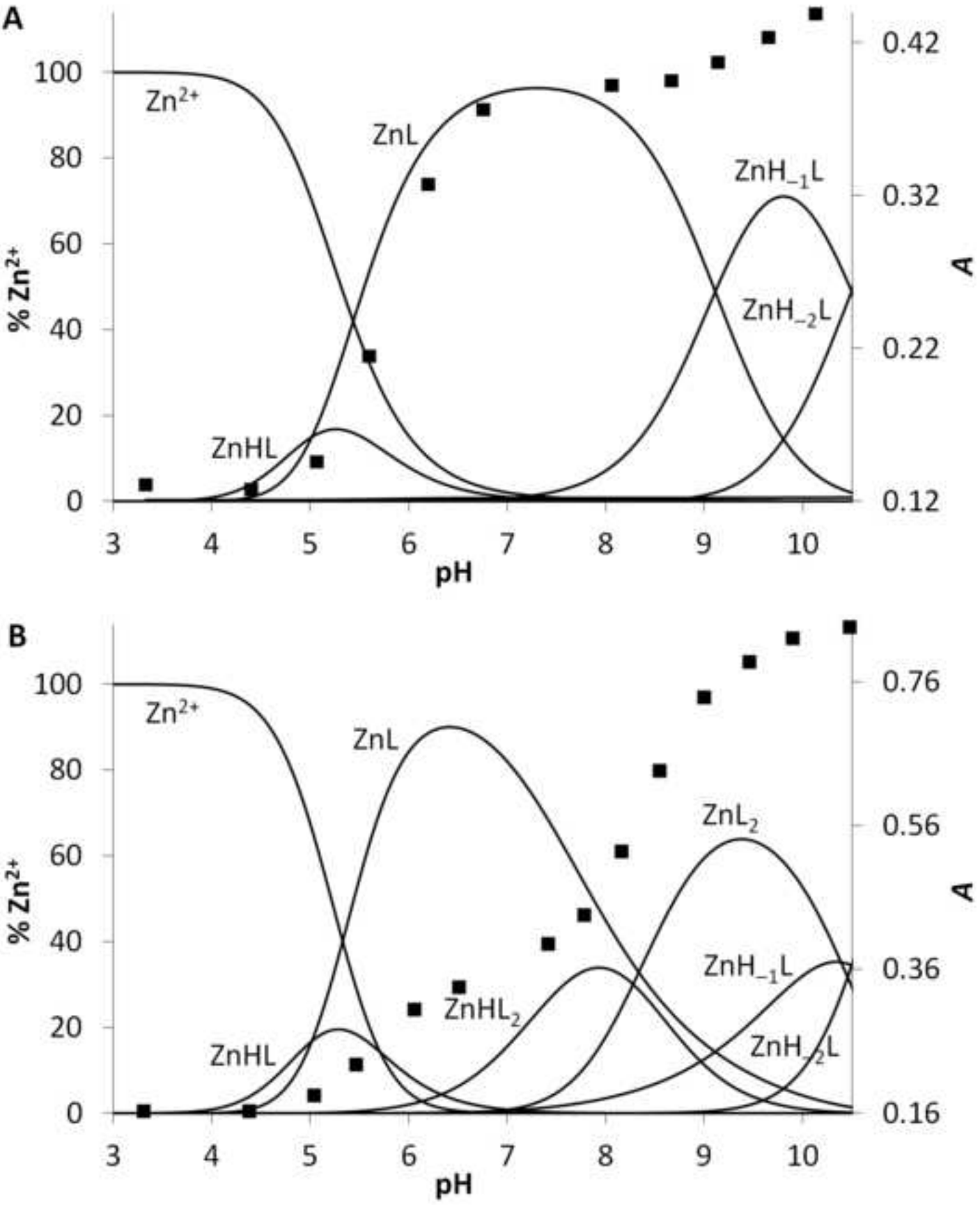

Fig_2

Click here to download high resolution image

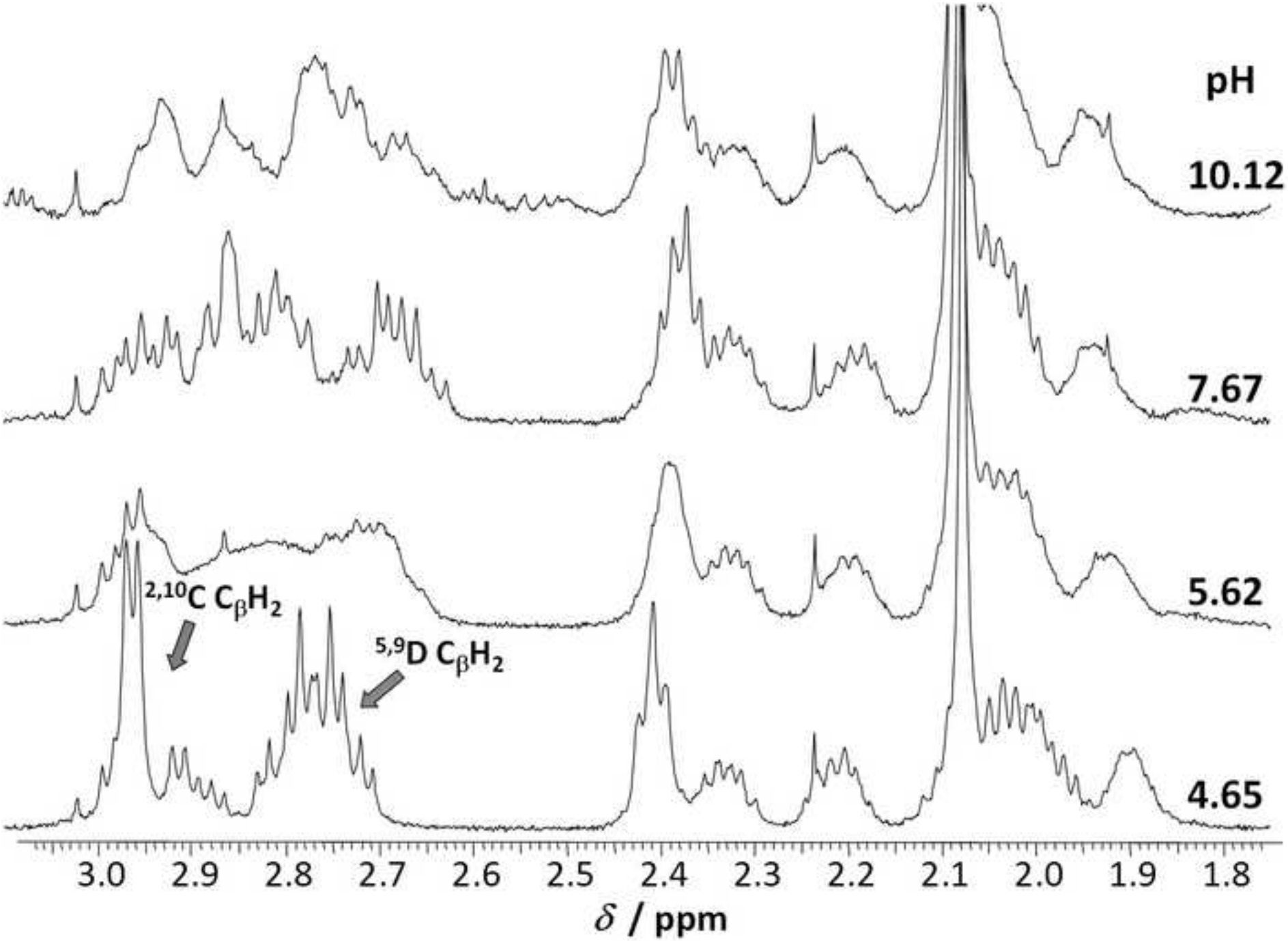

Fig_3

Click here to download high resolution image

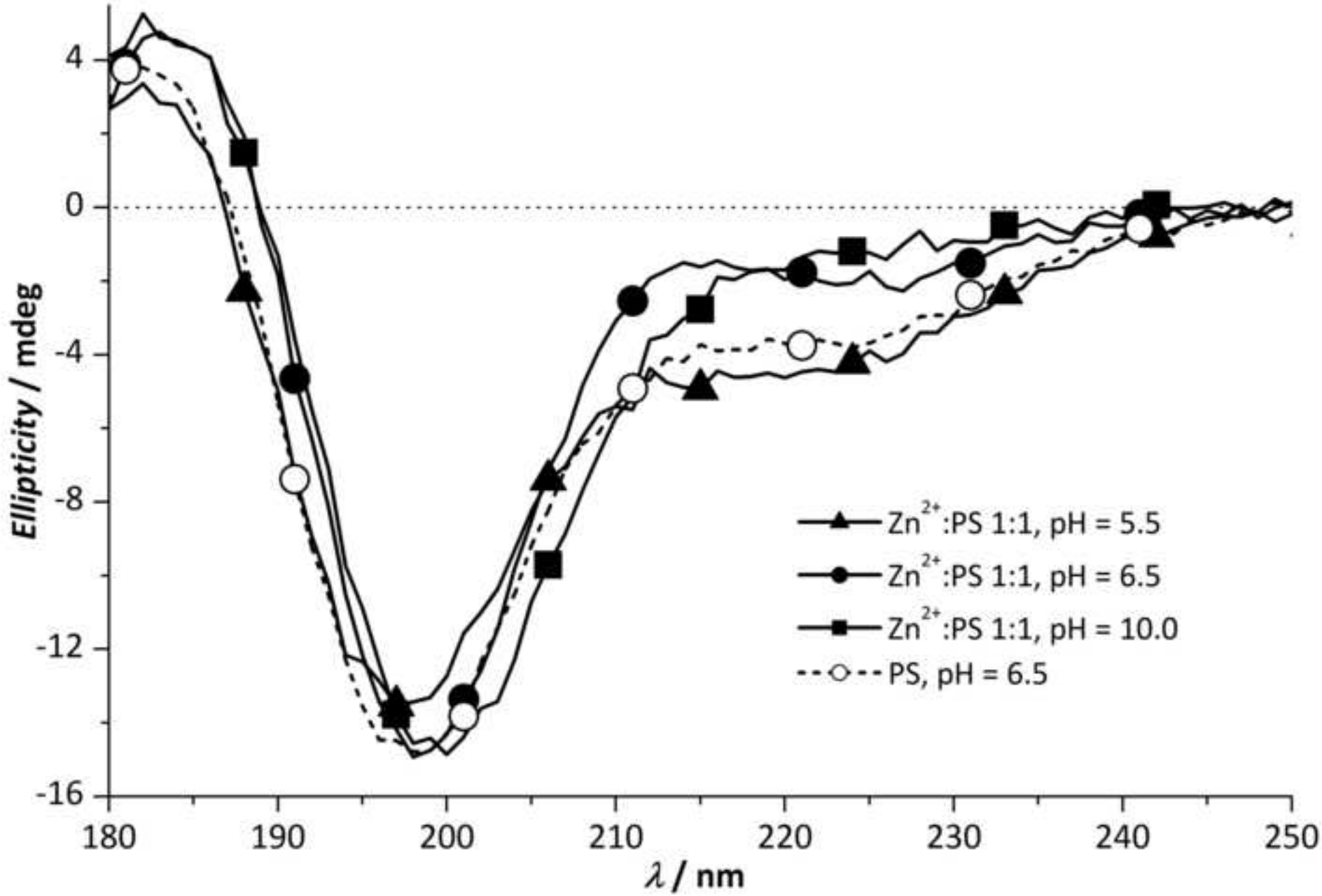

Fig_4

Click here to download high resolution image

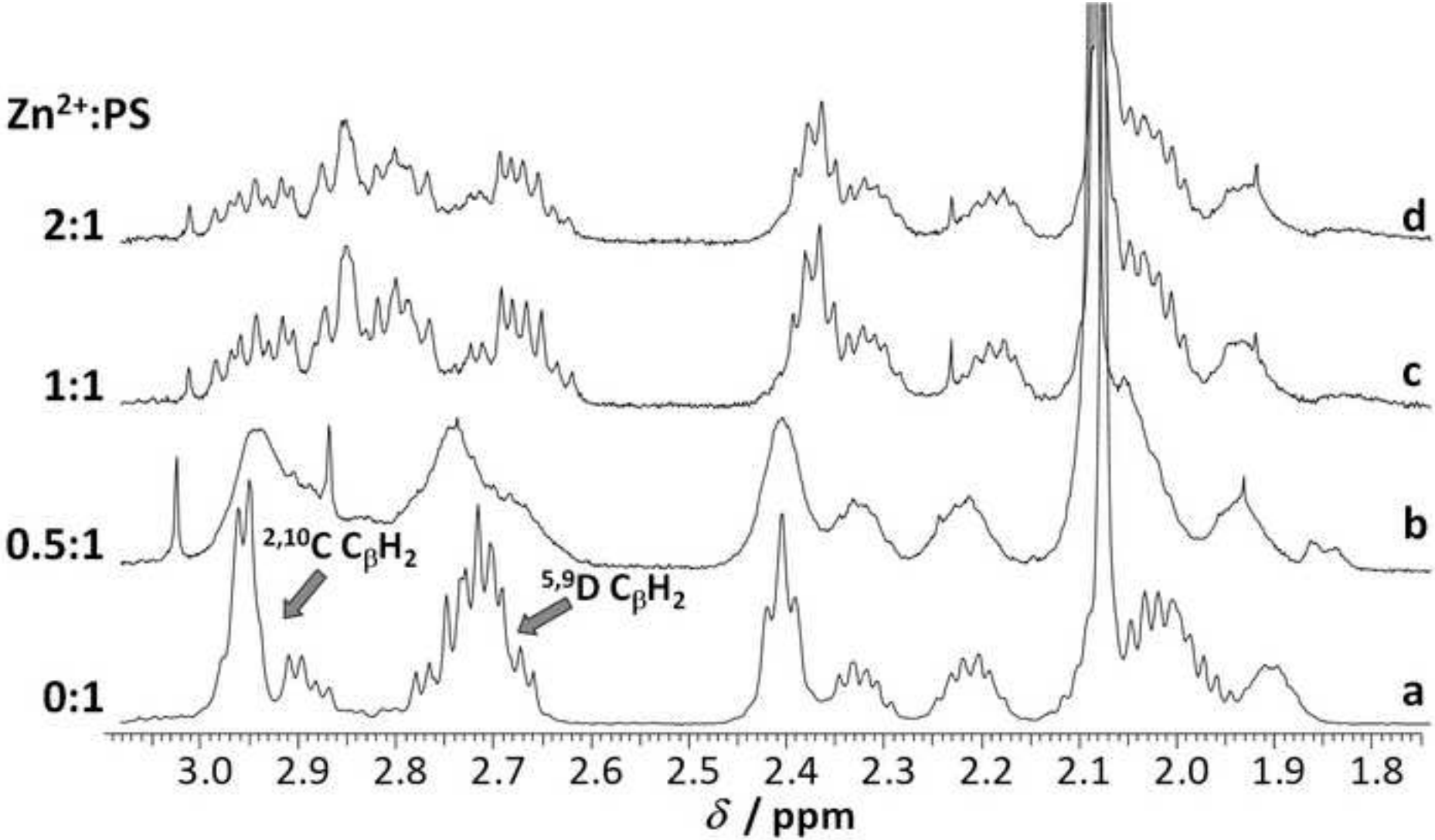

Fig_5

Click here to download high resolution image

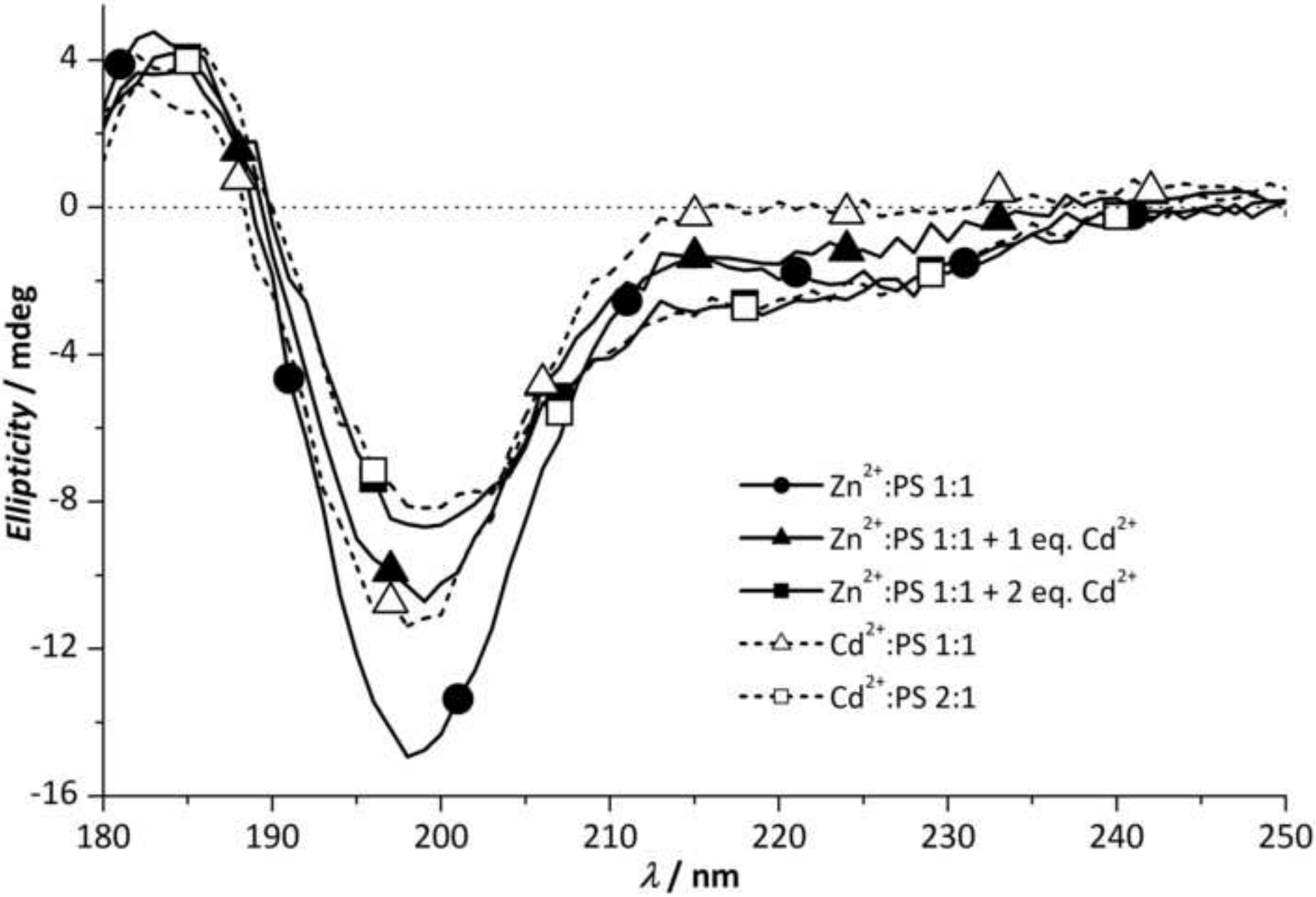

Fig_6

Click here to download high resolution image

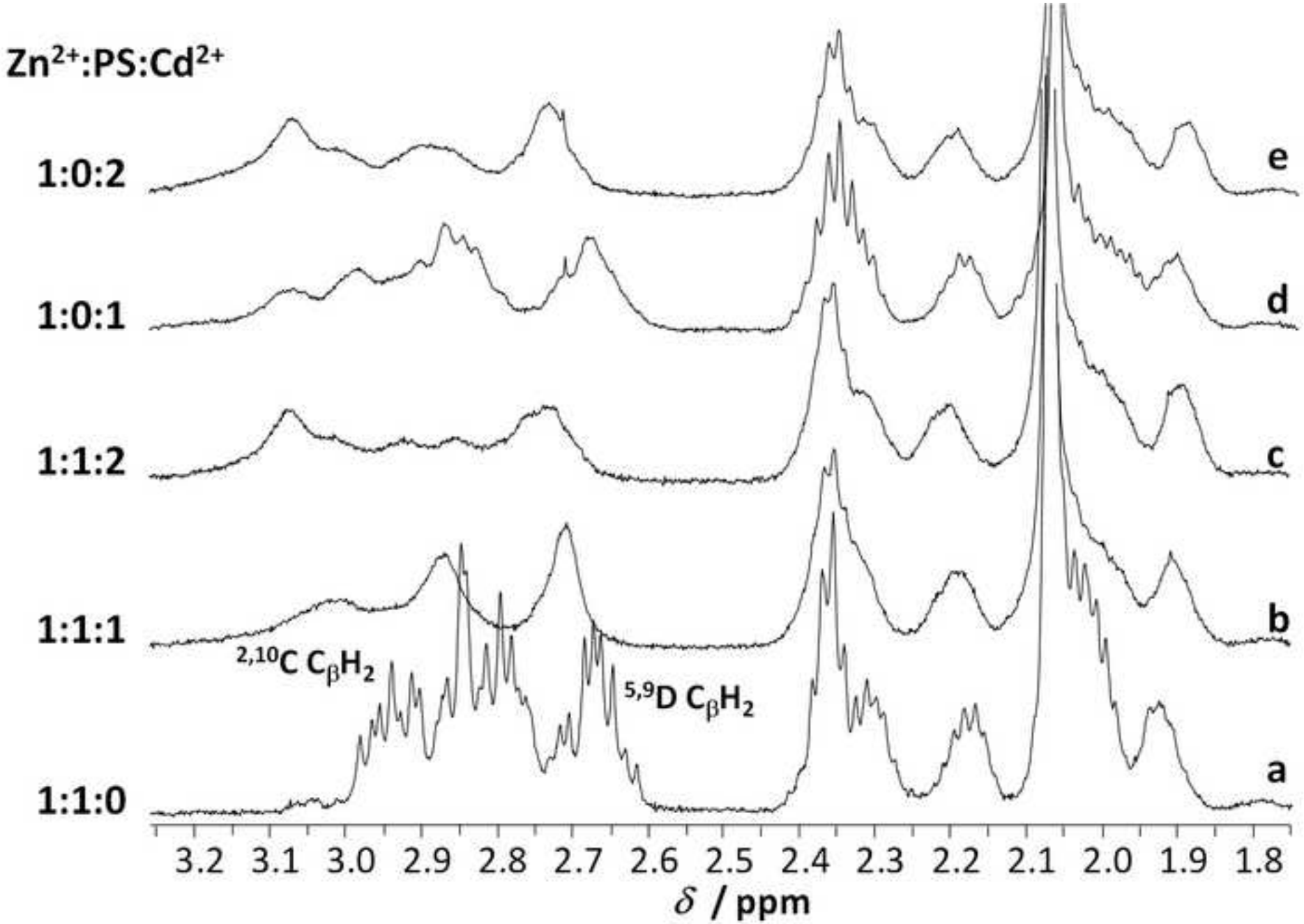

Fig_7

Click here to download high resolution image

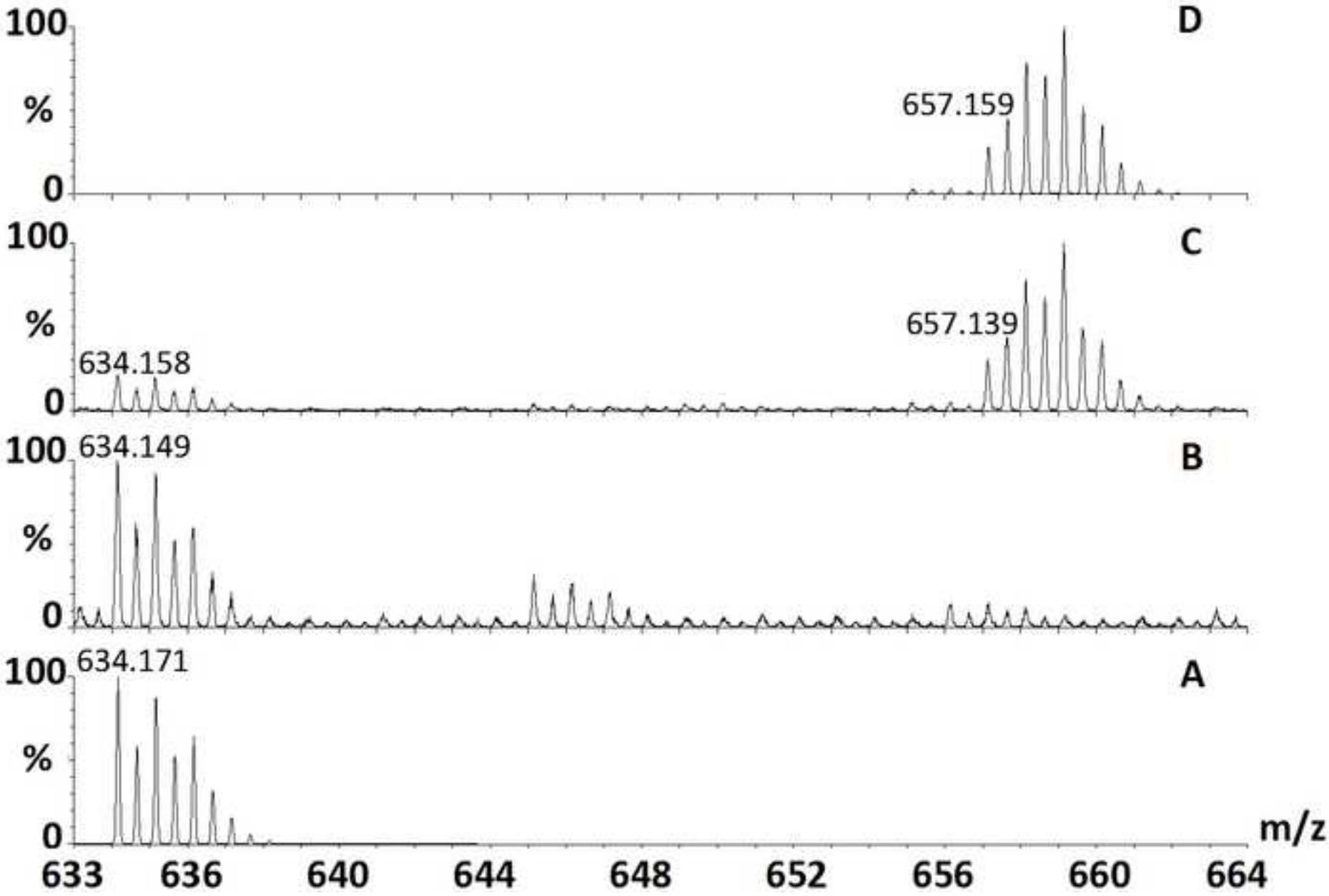

Fig_8

Click here to download high resolution image

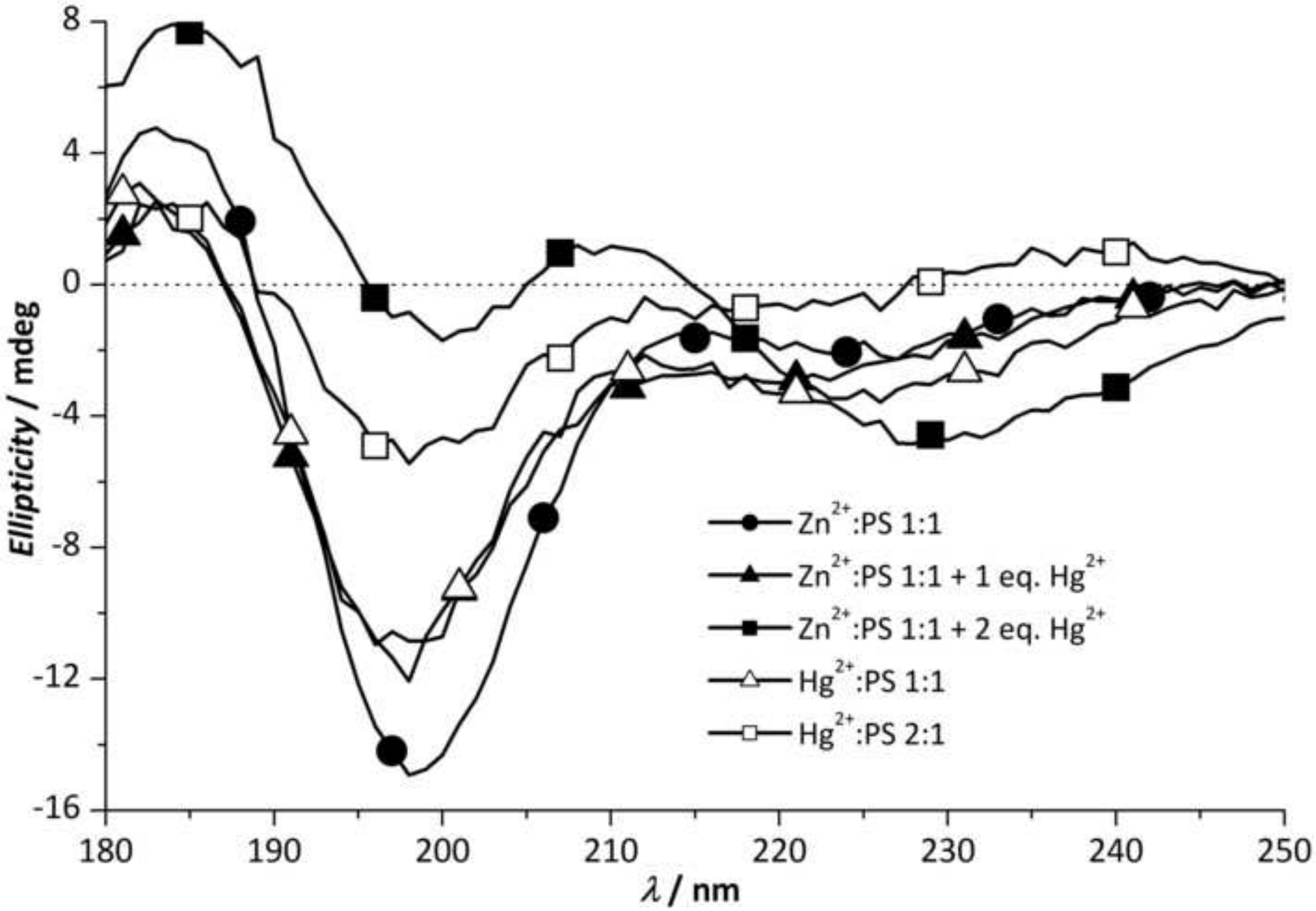

Fig_9

Click here to download high resolution image

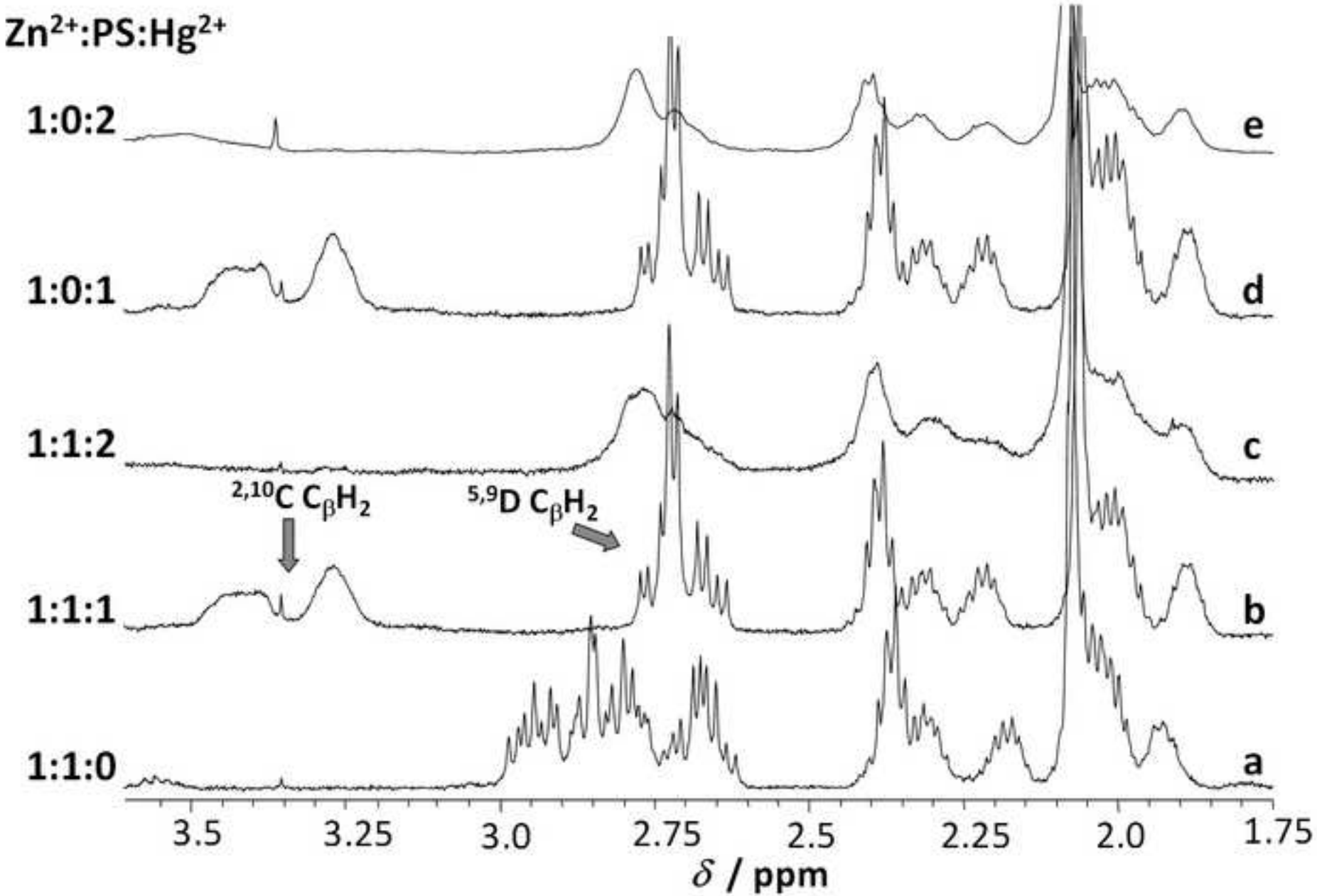

Supplementary material for:

Competition of zinc(II) with cadmium(II) or mercury(II) in binding to a 12-mer peptide

Attila Jancsó,* Béla Gyurcsik, Edit Mesterházy, Róbert Berkecz

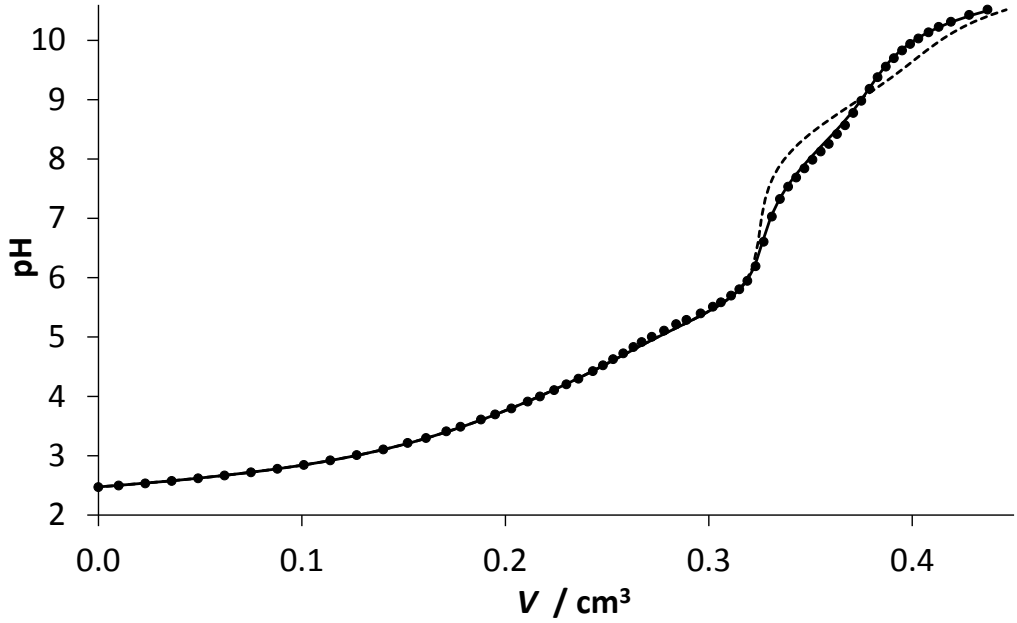

Fig. S1: Experimental titration data (circles) and the fit (solid line) of the zinc(II) : **PS** 0.5:1 system with the model presented in Table 1 ($c_{\mathbf{PS}}$ = 1.07×10^{-3} M, $c_{\mathbf{Zn^{2+}}}$ = 5.25×10^{-4} M, V_0 = 5.11 cm^3, I = 0.1 M $NaClO_4$, T = 298 K). The dashed line shows the best fit when the bis-complexes ($ZnHL_2$ and ZnL_2) are omitted from the model.

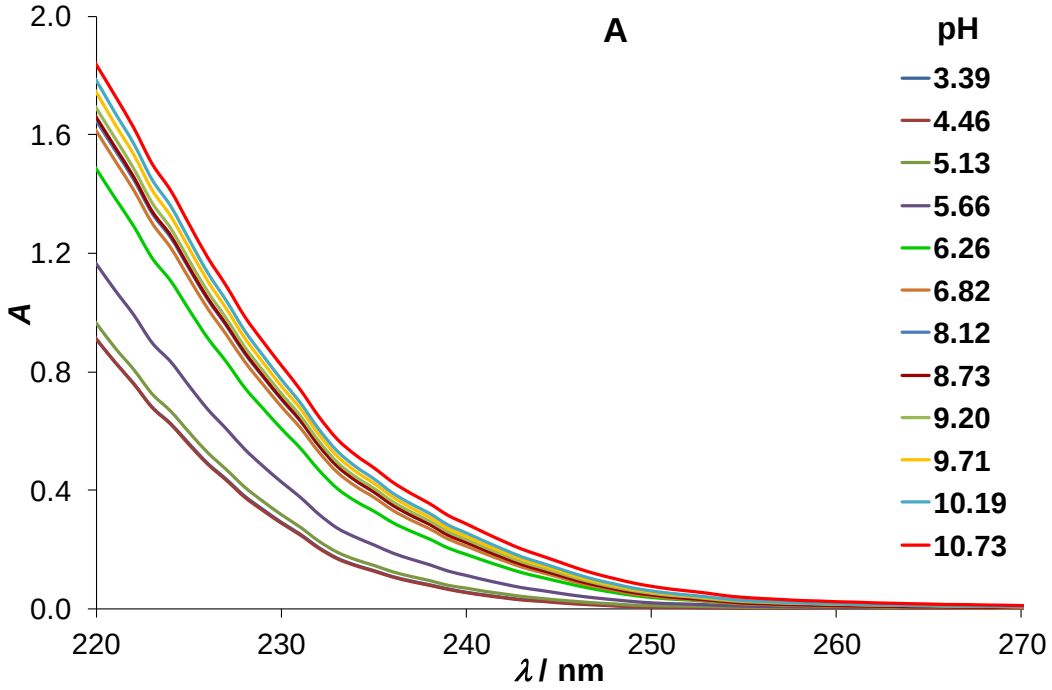

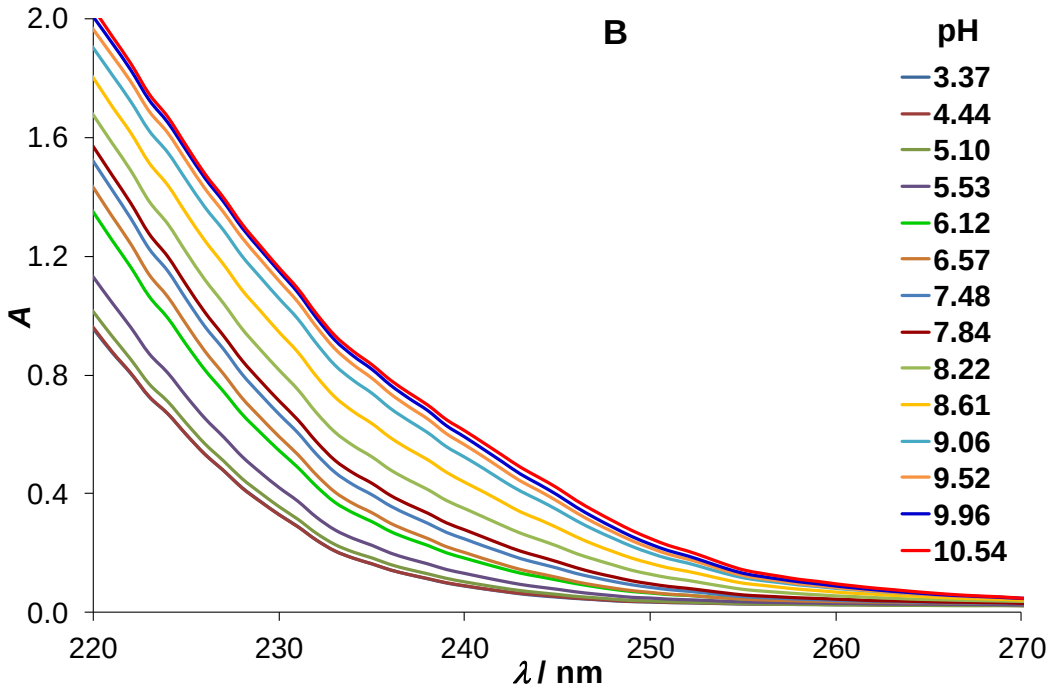

Fig. S2.A-B: pH-dependent UV spectra recorded in the zinc(II) – **PS** 1:1 (A), and 0.5:1 (B) systems ($c_{\mathbf{PS}}$ = 2.0×10^{-4} M (A,B), I = 0.1 M $NaClO_4$, T = 298 K, l = 0.5 cm).

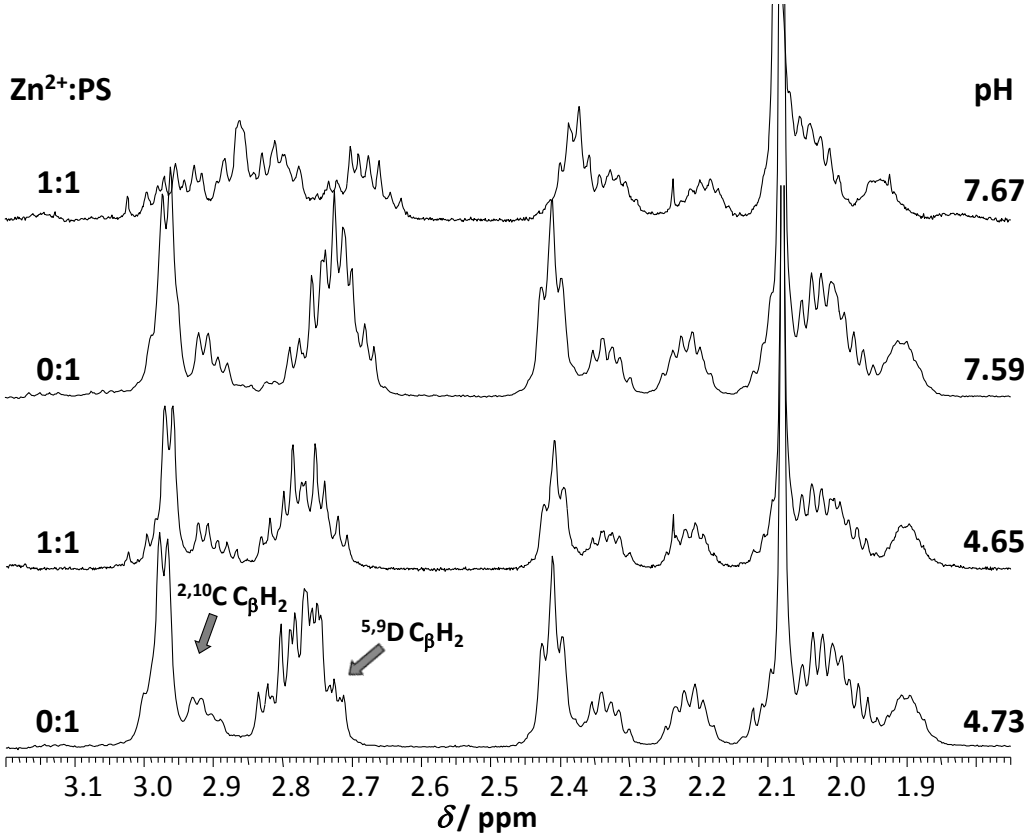

Fig. S3: Comparison of selected region of the ^{1}H NMR spectra of the peptide **PS** in the absence and presence of one equivalent of zinc(II) ions at pH ~ 4.7 and and pH ~ 7.6 ($c_{\mathbf{PS}}$ = 1.0×10^{-3} M, T = 298 K, 10 % w/w D_2O/H_2O).